On the Impact of Antenna Tilt on Cell-Free Systems Serving Ground Users and UAVs

Maria Clara R. Lobão, Wilker de O. Feitosa, Roberto P. Antonioli, Yuri C. B. Silva, Walter C. Freitas Jr., Gábor Fodor

***Abstract*— This work investigates the performance of cell-free multiple input multiple output systems serving ground user equipments (GUEs) and uncrewed aerial vehicles (UAVs) when varying the tilt angle of the access point antennas. The antenna tilt affects the radiation power pattern, such that tilting the antennas upwards is favourable for the UAVs, while tilting them downwards is favourable for the ground users. We study the performance of antenna tilting using uniform linear arrays and uniform planar arrays. Our results indicate that using a fixed downtilt favouring the ground users with the linear array arrangement is beneficial for the overall performance of the studied scenario. The reason behind this behavior is that UAVs are less penalized by slightly downtilting the arrays than terrestrial users by slightly uptilting the arrays. It is also observed that the impact of the array types depends on the ratio of UAVs in the system. Due to the high interference that UAVs cause on GUEs, when a lower UAV ratio is considered, the dimensional benefits of the planar array enhance their performance, degrading the GUEs; hence, in this case, the linear array presents fairer results, benefiting the whole system. For higher UAV ratios, however, the planar array achieves better sum rates.**

***Keywords*— Antenna tilt, cell-free systems, massive MIMO, UAV communications**

I. Introduction

For the 6th generation of mobile systems, distributed multiple input multiple output (MIMO) systems provide an efficient alternative to the conventional cellular architecture in terms of quality of service (QoS) and coverage, while benefiting from spatial diversity and multiplexing offered by the MIMO technology. Within the distributed MIMO (often referred to as 'cell-free') context, simultaneously serving aerial user devices, and specifically uncrewed aerial vehicles (UAVs), and terrestrial or ground user equipments (GUEs) has recently gained great interest in both academia and industry.

The advantages of using UAVs, due to their low-cost and high mobility attributes, have resulted in an increasing interest by industry, transport, monitoring and many other areas, motivating the studies on wireless communication networks with integrated UAVs [1], [2]. Recent works on cellular UAV communications have explored the impact of the antenna tilt angle (ATA) on the network performance when serving these equipments, given that usually the base station (BS) antennas are tilted downwards, as they are designed to prioritize the GUEs, and hence, the UAVs receive the data from the BS with slightly less power [3]. In [4], the trade-off offered by the downtilt angle of the antenna for the performance of coexisting UAVs and GUEs is analyzed. In [5], BSs with both uptilted and downtilted antennas serve coexisting UAVs and GUEs. In [3] and [6], the uptilt and downtilt of the antennas were explored on different exclusivity schemes of the BSs.

Concerning cell-free wireless networks serving UAVs, existing works have not devoted a particular attention to the model of the ATA [2], [7]. The current study seeks to investigate the link quality, in terms of spectral efficiency (SE), that a cell-free system provides to the entire network (GUEs and UAVs) with the antennas tilted up or down.

For scenarios with high data rate demands, such as in fifth generation (5G) and sixth generation (6G) networks, it is expected that the infrastructure of the communication system be able to provide and handle this requirement efficiently. Cell-free systems manage to provide high data rates for the users in uplink and downlink transmission [8], nonetheless, system attributes such as the array type can be manipulated in order to improve the QoS. The authors in [9] have worked on cell-free networks with correlated Rayleigh fading channels for two different types of arrays: uniform linear array (ULA) and uniform planar array (UPA). The addition of one dimension in the UPA arrangement improves the channel estimation and spectral efficiency due to the higher correlation factor in comparison to the ULA.

With this perspective, this present work investigates the performance of cell-free massive MIMO networks under Rician correlated fading channels, for systems with downtilt and uptilt angles under the employment of ULA and UPA. The main goal of this study is to compare these scenarios when serving both UAVs and GUEs in terms of mean user SE and sum SE. Simulations have shown that, while the uptilt benefits the UAVs, a fixed downwards ATA works better for the entire system. Moreover, the UPA arrangement presents an increase on the sum SE of the system. In Section II, scenario propagation, channel estimation and SE models are described. Section III shows the radiation power pattern used to model the antenna tilt of the antennas. Section IV presents the two antenna arrangements studied and their respective spatial correlation matrices, steering vectors and array factor

This work was supported in part by Ericsson Research, Technical Cooperation Contract UFC.50, in part by the Brazilian National Council for Scientific and Technological Development (CNPq), in part by the Coordenação de Aperfeiçoamento de Pessoal de Nível Superior - Brasil (CAPES) - Finance Code 001, and in part by CAPES/PRINT Grant 88887.311965/2018-00. G. Fodor was partially supported by the Celtic project 6G for Connected Sky, Project ID: C2021/1-9.

Maria Clara R. Lobão, Wilker de O. Feitosa, Roberto P. Antonioli, Yuri C. B. Silva, Walter C. Freitas Jr. are with the Wireless Telecommunications Research Group (GTEL), Federal University of Ceará (UFC), Fortaleza, Brazil. E-mails: {clara, wilker, antonioli, yuri, walter}@gtel.ufc.br. Gábor Fodor is with Ericsson Research and KTH Royal Institute of Technology, Stockholm, Sweden. (e-mails: gabor.fodor@ericsson.com, gaborf@kth.se).

for the total radiation pattern of the array. In Section V the simulation and numerical results are displayed and discussed. Finally, Section VI summarizes the conclusions of this work.

II. System Model

A cell-free network with L access points (APs) and K single-antenna user equipments (UEs) is considered. The UEs are divided into K_{GUE} GUEs and K_{UAV} UAVs, with $K = K_{\text{GUE}} + K_{\text{UAV}}$.

In order to model the ATA, this work uses the radiation power pattern of [10], also used in the 3rd Generation Partnership Project (3GPP) Technical Reports [11] and [12]. The horizontal pattern of this model is designed for a 3-sector cell. Thus, as a way to assure the coverage on the entire area, the APs are equipped each with $S = 3$ arrays of N antennas, with respective boresights distanced 120° from the others.

The APs are connected via fronthaul to a central processing unit (CPU). The system operates based on a time division duplex (TDD) protocol, and only the uplink (UL) transmission is evaluated. In this scenario, it is assumed that all the arrays at every AP serve all UEs.

A. Propagation Model

The link between UE and a receiver array at the AP is modeled following a Rician distribution. Similarly as in [2], the propagation channel $\mathbf{h}_{k,l,s} \in \mathbb{C}^N$ between the k-th UE and the s-th receiving array at the l-th AP is described with the expression:

$$\mathbf{h}_{k,l,s} = \left[\sqrt{\frac{\bar{K}_{k,l}}{\bar{K}_{k,l}+1}} \mathbf{a}_{k,l,s} + \sqrt{\frac{1}{\bar{K}_{k,l}+1}} \mathbf{h}^{(w)}_{k,l,s} \right] \sqrt{\beta_{k,l,s}}\,, \tag{1}$$

in which $\bar{K}_{k,l}$ represents the Rician K-factor, $\mathbf{h}^{(w)}_{k,l,s} \sim \mathcal{N}(0, \mathbf{R}_{k,l,s})$ is the non-line of sight (NLOS) Rayleigh term, with $\mathbf{R}_{k,l,s} \in \mathbb{C}^{N\times N}$ being the channel spatial correlation matrix, and $\mathbf{a}_{k,l,s}$ is the array steering vector. The component $\beta_{k,l,s}$ is the large-scale fading coefficient, describing the shadowing and the path-loss as:

$$\beta_{k,l,s} = 10^{\frac{PL_{k,l}+SH_{k,l}+G_{k,l,s}}{10}}\,, \tag{2}$$

where $PL_{k,l}$ is the path-loss in dB, $G_{k,l,s}$ is the receiver antenna gain in dB and $SH_{k,l}$ the correlated shadowing in dB, with standard deviation σ_{SH}, which changes when considering UAVs and GUEs for line of sight (LOS) and NLOS links. The steering vector, as well as the correlation matrix $\mathbf{R}_{k,l,s}$, is determined according to the antenna type, which will be described further in Section IV.

As described in [13], the link between the UE and the AP has a corresponding probability of LOS, which depends on the physical attributes of the setup, such as the horizontal distance between the two terminals and the height of the UAV. The path-loss and the Rician K-factor depend on this probability, given that both change for LOS and NLOS links. For an LOS channel, $\bar{K}_{k,l} = 15$ dB for UAVs and for GUEs, $\bar{K}_{k,l} \sim \mathcal{N}(5, 9)$ dB; for an NLOS channel, $\bar{K}_{k,l} = 0$ dB for all UEs. The probability of LOS, path-loss and Rician K-factor are modeled according to the urban micro (UMi) scenario in [12] and [11], for GUEs and UAVs, respectively.

B. Channel Estimation

The channel estimation is performed based on pilot transmission sent by the UEs. There are $\tau_p < K$ orthogonal pilot signals $\boldsymbol{\phi}_1, \ldots \boldsymbol{\phi}_{\tau_p}$ of length τ_p with $||\boldsymbol{\phi}_t||^2 = \tau_p$. As in [8], the signal at the receiver is correlated with the normalized pilot sequence sent by the UE, resulting in:

$$\mathbf{z}_{t_k,l,s} = \sum_{i\in\mathcal{P}_k} \sqrt{p_i \tau_p}\mathbf{h}_{i,l,s} + \mathbf{n}_{t_k,l,s}\,, \tag{3}$$

$\mathbf{z}_{t_k,l,s}$ is the received signal correlated with the pilot signal $\boldsymbol{\phi}_{t_k}$, t_k being the index of the pilot used by UE k, p_i is the transmitted power of the i-th UE, $\mathbf{n}_{t_k,l,s} \sim \mathcal{N}(0, \sigma^2\mathbf{I}_N)$ is the noise at the receiver and $\mathcal{P}_k$ is the set of UEs that use the same pilot. The minimum mean square error (MMSE) estimator is then applied, giving the channel estimate:

$$\hat{\mathbf{h}}_{k,l,s} = \sqrt{p_k\tau_p}\mathbf{R}_{k,l,s}\boldsymbol{\Psi}^{-1}_{t_k,l,s}\mathbf{z}_{t_k,l,s}\,, \tag{4}$$

with $\boldsymbol{\Psi}_{t_k,l,s} = \mathbb{E}\{\mathbf{z}_{t_k,l,s}\mathbf{z}^H_{t_k,l,s}\}$ and error $\tilde{\mathbf{h}}_{k,l,s} = \mathbf{h}_{k,l,s} - \hat{\mathbf{h}}_{k,l,s}$.

Given the limited number of pilot signals in the network, the choice of an appropriate pilot assignment method is imperative in order to minimize pilot contamination. For a scenario with both GUEs and UAVs, [13] shows that the "Scalable" pilot assignment represents the best trade-off in terms of SE for the UEs. This method is based on the initial access procedure of [14], in which the UE designates the AP with best large scale coefficient $\beta_{k,l,s}$ as its master AP, which in turn selects for the UE the pilot signal that causes the least pilot contamination.

C. Spectral Efficiency

The performance of the network in this work is evaluated by means of the SE. The channel estimates computed at the APs are sent to the CPU, which performs the decoding with large scale fading decoding (LSFD) weights [8]. Let us define $\mathbf{g}_{k,i} = \left[\mathbf{v}^H_{k,1,1}\mathbf{h}_{i,1,1}\ldots\mathbf{v}^H_{k,L,S}\mathbf{h}_{i,L,S}\right]^T$, where $\mathbf{v}_{k,l,s}$ is the MMSE combining vector[1] given by [8]:

$$\mathbf{v}_{k,l,s} = p_k\left(\sum_{i=1}^{K} p_i\left(\hat{\mathbf{h}}_{i,l,s}\hat{\mathbf{h}}^H_{i,l,s} + \mathbf{C}_{i,l,s}\right) + \sigma^2\mathbf{I}_N\right)^{-1}\hat{\mathbf{h}}_{k,l,s}\,, \tag{5}$$

with $\mathbf{C}_k = \text{diag}(\mathbf{C}_{k,1,1},\ldots,\mathbf{C}_{k,L,S})$ and $\mathbf{C}_{k,l,s} = \mathbb{E}\{\tilde{\mathbf{h}}_{k,l,s}\tilde{\mathbf{h}}^H_{k,l,s}\}$. The LSFD weights $\mathbf{w}_k$ that maximize the signal to interference-plus-noise ratios (SINRs) of the UEs can then be determined [8] :

$$\mathbf{w}_k = \left(\sum_{i=1}^{K} p_i\mathbb{E}\{\mathbf{g}_{k,i}\mathbf{g}^H_{k,i}\} + \sigma^2\mathbf{D}_k\right)^{-1}\mathbb{E}\{\mathbf{g}_{k,k}\}\,, \tag{6}$$

with $\mathbf{D}_k = \text{diag}\left(\mathbb{E}\{||\mathbf{v}_{k,1,1}||^2\}\ldots\mathbb{E}\{||\mathbf{v}_{k,L,S}||^2\}\right) \in \mathbb{C}^{LS\times LS}$.

Using (6), the maximum SINR is given by [8]:

$$\begin{aligned}\text{SINR}_k =& p_k\mathbb{E}\{\mathbf{g}^H_{k,k}\}\Bigg(\sum_{i=1}^{K} p_i\mathbb{E}\{\mathbf{g}_{k,i}\mathbf{g}^H_{k,i}\} + \sigma^2\mathbf{D}_k \\ &- p_k\mathbb{E}\{\mathbf{g}_{k,k}\}\mathbb{E}\{\mathbf{g}^H_{k,k}\}\Bigg)^{-1}\mathbb{E}\{\mathbf{g}_{k,k}\},\end{aligned} \tag{7}$$

[1]The combiner minimizes the conditional mean squared error given the estimated channel [8], [15].

allowing the computation of the achievable UL SE of UE k:

$$\mathrm{SE}_k = \left(1 - \frac{\tau_p}{\tau_c}\right) \log_2\left(1 + \mathrm{SINR}_k\right) , \tag{8}$$

where τ_c represents the coherence time length. Using (8), the sum SE of the system can be then defined as $\sum_{k=1}^{K} \mathrm{SE}_k$.

III. Radiation Pattern

The antenna gain can be generated according to the model in [10]. The vertical radiation pattern is dependent on the antenna tilt angle and given by:

$$G_V(\theta, \theta_{\text{tilt}}) = -\min\left[12\left(\frac{\theta - \theta_{\text{tilt}}}{\theta_{\text{3dB}}}\right)^2, A_m\right] , \tag{9}$$

in which $\theta \in [-\pi, \pi]$ is the elevation angle of incidence of the incoming wave at the receiving element, θ_{tilt} is the antenna tilt angle and θ_{3dB} is the half power beamwidth (HPBW) of the vertical pattern, with value $\theta_{\text{3dB}} = 15°$ as in [10]. The component A_m is the maximum attenuation of the antenna gain, assumed to be 20 dB in [10].

The horizontal antenna gain is given by the expression:

$$G_H(\gamma) = -\min\left[12\left(\frac{\gamma}{\gamma_{\text{3dB}}}\right)^2, A_m\right] , \tag{10}$$

where $\gamma \in \left[-\frac{\pi}{2}, \frac{\pi}{2}\right]$ is the azimuth angle of incidence of the incoming wave and γ_{3dB} is the HPBW of the horizontal pattern, with value $\gamma_{\text{3dB}} = 70°$ in [10]. Using (9) and (10), the 3D antenna radiation power pattern of the element is:

$$G_E(\theta, \gamma, \theta_{\text{tilt}}) = -\min\left[-\left(G_V(\theta, \theta_{\text{tilt}}) + G_H(\gamma)\right), A_m\right] . \tag{11}$$

The tilt angle can vary in the interval $\left[-\frac{\pi}{2}, \frac{\pi}{2}\right]$. The negative values in the range are associated with the uptilt of the antenna, while the positive ones represent the downtilt.

As described in [16], when using identical elements, the total radiation pattern of the array is given by the product of the element pattern to the Array Factor (AF). In dB, the radiation pattern of the array is:

$$G_A(\theta, \gamma, \theta_{\text{tilt}}) = G_E(\theta, \gamma, \theta_{\text{tilt}}) + 10\log_{10} AF(\theta, \gamma) . \tag{12}$$

Hence, the antenna gain at the s-th array of the l-th AP for the k-th UE is determined by (12) as $G_{k,l,s} = G_A(\theta_{k,l,s}, \gamma_{k,l,s}, \theta_{\text{tilt}})$.

The array factor is a function of the array physical arrangements, such as spacing, number of antennas, relative phases and magnitudes, therefore, its expression changes depending on the type of array being used. The AF for the considered array configurations in this study are given in Section IV.

IV. Antenna Arrangement

In this work, two antenna array types are considered: ULA and UPA. As expressed in [9], the UPA configuration shows an improved performance in detriment of the ULA for cell-free systems as a consequence of its beneficial spatial characteristics. Therefore, this study seeks to compare the performance of these two array configurations for a cell-free network serving GUEs and UAVs.

As mentioned in Sections II and III, the main features affected by the antenna type are the steering vector $\mathbf{a}_{k,l,s}$, the spatial correlation matrix $\mathbf{R}_{k,l,s}$, and the array factor AF, described for each configurations as follows:

1) ULA: For the ULA type case, the elements are disposed uniformly with spacing d. The correlation matrix is generated according to the local scattering spatial correlation model in [8], which designs $\mathbf{R}^{\text{ULA}}_{k,l,s} \in \mathbb{C}^{N\times N}$ as a Toeplitz matrix that describes the macroscopic effects of the channel.

As for the steering vector $\mathbf{a}_{k,l,s}$ in (13), the element a_n for the n-th antenna of the s-th array on AP l in (13) depends on the Angle of Arrival (AoA) $\gamma_{k,l,s}$ of the corresponding UE:

$$\mathbf{a}_{k,l,s} = \left[a_1, \ldots, a_N\right]^T , a_n = e^{-j\frac{2\pi}{\lambda}(n-1)d\sin\gamma_{k,l,s}} . \tag{13}$$

The array factor for the ULA configuration is given as in [16] for a linear array along the x axis starting at the origin:

$$AF(\theta, \gamma) = \frac{1}{N}\sum_{n=1}^{N} e^{j\frac{2\pi}{\lambda}(n-1)d\sin\theta\cos\gamma} , \tag{14}$$

where it is given the same weight $\frac{1}{N}$ for all the elements and no phase excitation difference is considered.

2) UPA: For the UPA case, the Kronecker-type approximation in [17] is used to compute the correlation matrix. In this approximation, the matrix $\mathbf{R}^{\text{UPA}}_{k,l,s} \in \mathbb{C}^{N\times N}$ is determined through the Kronecker product of the correlation matrices of orthogonal ULAs.

Assuming a UPA lying on the xy plane, with dimensions $M_x \times M_y$, $M_xM_y = N$, in which the adjacent elements have the same spacing d, the following Toeplitz matrices can be defined: $\mathbf{R}^{\text{ULA}_x}_{k,l,s} \in \mathbb{C}^{M_x\times M_x}$ for the elements in the x axis and $\mathbf{R}^{\text{ULA}_y}_{k,l,s} \in \mathbb{C}^{M_y\times M_y}$ for the elements in the y axis. Assuming also that the correlation in each axis does not depend on the other, the UPA correlation matrix is defined as $\mathbf{R}^{\text{UPA}}_{k,l,s} = \mathbf{R}^{\text{ULA}_x}_{k,l} \otimes \mathbf{R}^{\text{ULA}_y}_{k,l,s}$, and has a Toeplitz structure.

Regarding the steering vector, the design of the phase shifts depends on both the azimuth AoA $\gamma_{k,l,s}$ and the elevation AoA $\theta_{k,l,s}$. Determining the vectors:

$$\mathbf{a}^x_{k,l,s} = \left[u^1_{k,l,s} \ldots u^{M_x}_{k,l,s}\right]^T , \tag{15}$$

$$\mathbf{a}^y_{k,l,s} = \left[v^1_{k,l,s} \ldots v^{M_y}_{k,l,s}\right]^T , \tag{16}$$

where

$$u^{m_x}_{k,l,s} = e^{j\frac{2\pi}{\lambda}(m_x-1)d\sin\theta_{k,l,s}\cos\gamma_{k,l,s}} , \tag{17}$$

$$v^{m_y}_{k,l,s} = e^{j\frac{2\pi}{\lambda}(m_y-1)d\sin\theta_{k,l,s}\sin\gamma_{k,l,s}} , \tag{18}$$

with $m_x = 1, \ldots, M_x$ and $m_y = 1, \ldots, M_y$, the steering vector is calculated as:

$$\mathbf{a}_{k,l,s} = \mathbf{a}^x_{k,l,s} \otimes \mathbf{a}^y_{k,l,s} . \tag{19}$$

For the UPA configuration, the array factor will be given as [16]:

$$AF(\theta, \gamma) = \frac{1}{M_xM_y}\sum_{m_x=1}^{M_x}\sum_{m_y=1}^{M_y} e^{j\frac{2\pi}{\lambda}d\alpha_{x,y}} , \tag{20}$$

$$\alpha_{x,y} = (m_x - 1)\sin\theta\cos\gamma + (m_y - 1)\sin\theta\sin\gamma ,$$

in which, as well as for the ULA, the same weight $\frac{1}{M_x M_y}$ is considered for all the elements and no phase excitation difference is considered.

V. Simulation and Results

The cell-free scenarios studied in this work were simulated using Python3. The results were obtained through the analysis of the system UL SE of (8) under different tilt angles and distinct antenna arrangements. 200 Monte Carlo simulations were performed, where the UEs were randomly positioned withing the simulation area while the APs were distributed uniformly. The averaging of the SINR was taken over 200 channel realizations.

The deployment of the UEs on the system was done considering $K = 40$ UEs, being $K_{\text{GUE}} = 32$ and $K_{\text{UAV}} = 8$, corresponding to a 25% UAV/GUE ratio (case 4 in [11]); the UEs transmit the pilot signals with full power. The UEs were served simultaneously by $L = 100$ APs, each equipped with 3 arrays of $N = 4$ elements, which means for the UPA $M_x = M_y = 2$; the tilt angle on the arrays θ_{tilt} is fixed for the entire network. Table I shows the other parameters used in this work for the simulation of the system and propagation model.

TABLE I

Simulation Parameters.

Parameter	Value
Carrier frequency	f_c = 2 GHz
Communication bandwidth	W = 20 MHz
GUE and AP heights	1.5 m, 11.5 m
UAV height	uniform, $[23, 230]$ m
UL power per UE	p_k = 100 mW
Antenna spacing	$d = (1/2)\,\lambda$
Number of pilots	τ_p = 10
Coherence block length	τ_c = 200
GUEs σ_{sh} (LOS, NLOS)	4, 8.2
UAVs σ_{sh} (LOS [11], NLOS)	$\max(2, 5e^{h_{\text{UAV}}/100})$, 8

Figure 1 shows the mean SE of UAVs and GUEs as a function of the ATA θ_{tilt}, which in this case is varying from $-20°$ to $20°$. It can be observed that, as expected, the SE of the UAVs benefits from the negative angles, that represent the uptilt of the antenna, while the SE of the GUEs is strengthened by the positive angles, representing the downtilt. In each of these cases, one type of UEs is prioritized in detriment of the other, achieving their respective maximum mean SE. Figure 1a also shows that for higher values of θ_{tilt} in the positive direction, the UAVs mean SE lightly increases again, while the GUEs mean SE decreases in Figure 1b. A reflected behavior can be noticed for the most negative values. It can be concluded that, as the antenna is inclined on a more accentuated angle, the system stops serving the UEs with higher power as the main beam of the radiation pattern in (9) covers a smaller area; the same can be said about the far negative values.

Moreover, as explained in [13], due to better propagation conditions, the UAVs SE increases significantly, resulting in more interference power on the GUEs SINR, degrading the channel estimates and SE, consequently. This explains why the mean SE of the UAVs increases as the GUEs decreases when the coverage is impaired by the higher ATAs.

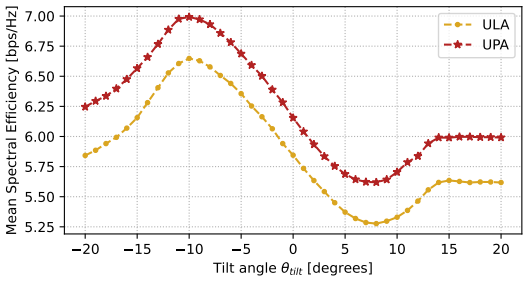

(a) Mean SE of UAVs.

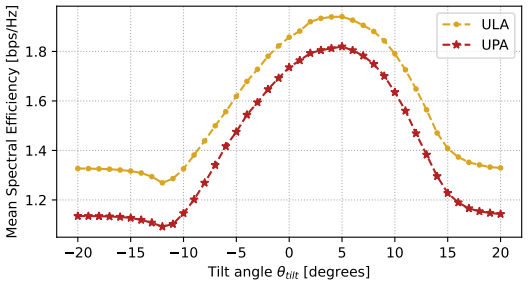

(b) Mean SE of GUEs.

Fig. 1. Mean SE in terms of the antenna tilt angle on ULA and UPA arrangements for UAVs and GUEs.

Figure 1 also considers both antenna arrangements studied in this paper. It is important to notice that, as Figure 1a shows, for UAVs, the employment of a UPA configuration is highly favorable, however, the SE of the GUEs is diminished as a consequence. Again, the superior environment traits and propagation conditions of the UAVs, empowered by the use of an array architecture that improves the spatial attributes of the network, decreases the overall performance of the transmission for GUEs.

Even with the disparity of values, the relative behavior of the mean SE in terms of the ATA is similar for both antenna arrangements. Approximately the same tilt angle gives the maximum mean SE for each type of UE: $\theta_{\text{tilt}} = -10°$ for UAVs and $\theta_{\text{tilt}} = 5°$ for GUEs. In order to investigate the performance of the entire system under ULA and UPA arrangements, the sum SE of the scenarios for each array configuration and tilt value is taken.

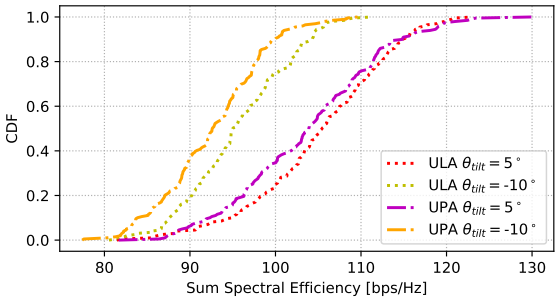

Fig. 2. CDF of the Sum SE for system with ULA, UPA and with the fixed optimal tilt angles for GUEs and UAVs.

The results of these scenarios are shown in Figure 2. The curves show that, in this case, the employment of a downtilt prioritizing the GUEs is more beneficial for the system as a whole than when focusing on the UAVs. This is due to the fact

that the UAVs already have good rates and higher SE than the GUEs; when the antenna is tilted downwards, the benefits for GUEs are more significant than the impairments on UAVs.

When focusing on the performance of the systems for each array type, it can be seen that, as expected from [9], the UPA does present a slight benefit to the network, given that it provides higher SE for the best UEs. Nonetheless, the ULA arrangement outperforms the UPA in overall sum performance for both downtilt and uptilt scenarios, given that, although the UPAs achieve higher rates, they benefit more the UAVs in detriment of the GUEs, decreasing their SE, and, as a consequence, the sum SE of the entire system.

It is important to notice that these results are related to the ratio of UAVs in the system. Increasing the number of UAVs of the scenario impacts on the Sum SE dynamic shown in Figure 2. Figure 3 presents the CDF of the Sum SE for cell-free systems with $K_{\text{UAV}} = 16$ and $K_{\text{GUE}} = 24$, maintaining $K = 40$, and the tilt angles of the arrays are the same as for the scenario of Figure 2. Unlike the previous results, employing the UPA prioritizing the GUEs is better for the system. Since $K_{\text{UAV}} > \tau_p$, the pilot contamination between UAVs is increased and, given their better propagation conditions, so is the overall system interference. The UPA, due to its spatial benefits, combined with the downtilt, results in the GUEs being less penalized than the UAVs, as it increases their SE even in the presence of the UAVs interfering signals. Analyzing the scenarios for both arrangements, the UPA outperforms the ULA even when the array is tilted upwards, and the performance disparity of each arrangement with up and down tilt is less accentuated.

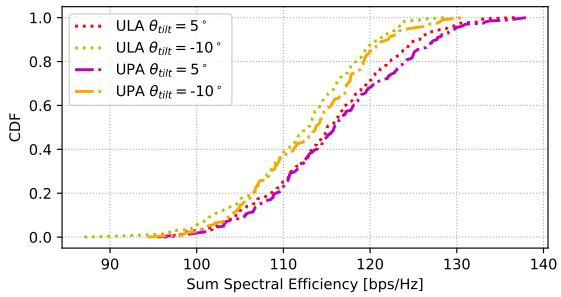

Fig. 3. CDF of the Sum SE for system with ULA, UPA and with the fixed optimal tilt angles for higher number of UAVs.

VI. Conclusions

In this work, the performance of cell-free systems serving both UAVs and GUEs in scenarios with different antenna tilt angles and antenna array configurations was investigated. The results indicate that, while uptilt angles benefit the UAVs, in a scenario, where all the antennas apply the same tilt, a downwards angle prioritizing the GUEs is best for the entire system, given that the loss of SE for the UAVs is not significant compared to the GUEs gain. Regarding the antenna arrangements, it was concluded that in spite of the fact that the UPA arrangement offers a higher spatial control on the transmission, the improvements of this arrangement are noticed only by the UAVs, that with better propagation conditions achieve higher SE and better estimates, causing more interference for the GUEs. In contrast, the ULA arrangement showed better performance in terms of sum SE. Combined with the downtilt angle, it achieved the highest overall rates when compared to the UPAs, for the 25% UAV/GUE ratio. When considering a higher ratio, the results showed that the use of a UPA arrangement works best for the system, while still prioritizing the GUEs in order to increase their SE. As future works, dedicated networks with combined uptilt and downtilt can be explored.

References

[1] G. Geraci, A. Garcia-Rodriguez, L. Galati Giordano, D. López-Pérez, and E. Björnson, "Understanding UAV cellular communications: From existing networks to massive MIMO," *IEEE Access*, vol. 6, pp. 67 853–67 865, 2018. DOI: 10.1109/ACCESS.2018.2876700.

[2] C. D'Andrea, A. Garcia-Rodriguez, G. Geraci, L. G. Giordano, and S. Buzzi, "Analysis of uav communications in cell-free massive mimo systems," *IEEE Open Journal of the Communications Society*, vol. 1, pp. 133–147, 2020. DOI: 10.1109/OJCOMS.2020.2964983.

[3] S. Kim, M. Kim, J. Y. Ryu, and J. Lee, "Impact of base station antenna tilt angle on UAV communications," in *GLOBECOM 2020 - 2020 IEEE Global Communications Conference*, 2020, pp. 01–06. DOI: 10.1109/GLOBECOM42002.2020.9322137.

[4] R. Amer, W. Saad, and N. Marchetti, "Toward a connected sky: Performance of beamforming with down-tilted antennas for ground and UAV user co-existence," *IEEE Communications Letters*, vol. 23, no. 10, pp. 1840–1844, 2019. DOI: 10.1109/LCOMM.2019.2927452.

[5] Y. Du, H. Zhang, and J. Peng, "Modeling and coverage analysis for cellular-connected UAVs with up-tilted antenna," *IEEE Communications Letters*, vol. 26, no. 11, pp. 2572–2575, 2022. DOI: 10.1109/LCOMM.2022.3188683.

[6] S. Kim, M. Kim, J. Y. Ryu, J. Lee, and T. Q. S. Quek, "Non-terrestrial networks for UAVs: Base station service provisioning schemes with antenna tilt," *IEEE Access*, vol. 10, pp. 41 537–41 550, 2022. DOI: 10.1109/ACCESS.2022.3166241.

[7] J. Zheng, J. Zhang, and B. Ai, "Uav communications with wpt-aided cell-free massive mimo systems," *IEEE Journal on Selected Areas in Communications*, vol. 39, no. 10, pp. 3114–3128, 2021. DOI: 10.1109/JSAC.2021.3088632.

[8] Ö. T. Demir, E. Björnson, and L. Sanguinetti, "Foundations of user-centric cell-free massive MIMO," *Foundations and Trends in Signal Processing*, vol. 14, no. 3-4, pp. 162–472, 2021.

[9] J. Amadid, A. Belhabib, A. Khabba, A. Zeroual, and M. M. Hassani, "On channel estimation and spectral efficiency for cell-free massive mimo with multi-antenna access points considering spatially correlated channels," *Transactions on Emerging Telecommunications Technologies*, vol. 33, no. 5, e4438, 2022. DOI: https://doi.org/10.1002/ett.4438.

[10] ITU-R, "Guidelines for evaluation of radio interface technologies for IMT-advanced," International Telecommunications Union - Radiocommunications Sector (ITU-R), Tech. Rep., Dec. 2009.

[11] 3GPP, "Enhanced LTE support for aerial vehicles," 3rd Generation Partnerhsip Project, TR 36.777, Jan. 2018, v.15.0.0.

[12] 3GPP, "Study on channel model for frequencies from 0.5 to 100 GHz," 3rd Generation Partnership Project, TR 38.901, Mar. 2022, v.17.0.0.

[13] M. C. R. Lobão, W. O. Feitosa, R. P. Antonioli, *et al.*, "Pilot assignment for cell-free systems serving ground users and unmanned aerial vehicles," *XL Simpósio Brasileiro de Telecomunicações e Processamento de Sinais*, 2022. DOI: 10.14209/sbrt.2022.1570824562.

[14] E. Björnson and L. Sanguinetti, "Scalable cell-free massive MIMO systems," *IEEE Trans. Commun.*, vol. 68, no. 7, pp. 4247–4261, Jul. 2020. DOI: 10.1109/tcomm.2020.2987311.

[15] G. Fodor, P. D. Marco, and M. Telek, "On minimizing the mse in the presence of channel state information errors," *IEEE Communications Letters*, vol. 19, no. 9, pp. 1604–1607, 2015. DOI: 10.1109/LCOMM.2015.2449317.

[16] C. Balanis, *Antenna Theory: Analysis and Design*. Wiley, 2015, ISBN: 9781119178996.

[17] J. Li, X. Su, J. Zeng, *et al.*, "Codebook design for uniform rectangular arrays of massive antennas," in *2013 IEEE 77th Vehicular Technology Conference (VTC Spring)*, 2013, pp. 1–5. DOI: 10.1109/VTCSpring.2013.6692478.